9764 *Biochemistry* **2009,** *48,* 9764–9774
DOI: 10.1021/bi901409g

BIOCHEMISTRY
including biophysical chemistry & molecular biology
Article

An Oxygen-Sensing Diguanylate Cyclase and Phosphodiesterase Couple for c-di-GMP Control[†]

Jason R. Tuckerman,[‡] Gonzalo Gonzalez,[‡] Eduardo H. S. Sousa,[§] Xuehua Wan,[∥] Jennifer A. Saito,[∥] Maqsudul Alam,[∥,⊥] and Marie-Alda Gilles-Gonzalez*[,‡]

[‡]*Department of Biochemistry, University of Texas Southwestern Medical Center, 5323 Harry Hines Boulevard, Dallas, Texas 75390-9038,* [§]*Department of Organic and Inorganic Chemistry, Federal University of Ceara, Center for Sciences, CEP 60455-760 Fortaleza-Ceara, Brazil,* [∥]*Department of Microbiology, University of Hawaii, 2538 The Mall, Snyder Hall 207, Honolulu, Hawaii 96822, and* [⊥]*Centre for Chemical Biology, Persiaran Bukit Jambul, 11900 Bayan Lepas, Penang, Malaysia*

Received August 12, 2009; Revised Manuscript Received September 16, 2009

ABSTRACT: A commonly observed coupling of sensory domains to GGDEF-class diguanylate cyclases and EAL-class phosphodiesterases has long suggested that c-di-GMP synthesizing and degrading enzymes sense environmental signals. Nevertheless, relatively few signal ligands have been identified for these sensors, and even fewer instances of *in vitro* switching by ligand have been demonstrated. Here we describe an *Escherichia coli* two-gene operon, *dosCP*, for control of c-di-GMP by oxygen. In this operon, the gene encoding the oxygen-sensing c-di-GMP phosphodiesterase *Ec* Dos (here renamed *Ec* DosP) follows and is translationally coupled to a gene encoding a diguanylate cyclase, here designated DosC. We present the first characterizations of DosC and a detailed study of the ligand−dose response of DosP. Our results show that DosC is a globin-coupled sensor with an apolar but accessible heme pocket that binds oxygen with a K_d of 20 μM. The response of DosP activation to increasing oxygen concentration is a complex function of its ligand saturation such that over 80% of the activation occurs in solutions that exceed 30% of air saturation (oxygen $> 75\ \mu$M). Finally, we find that DosP and DosC associate into a functional complex. We conclude that the *dosCP* operon encodes two oxygen sensors that cooperate in the controlled production and removal of c-di-GMP.

The relatively recently discovered dinucleotide 3′−5′ cyclic diguanylic acid (c-di-GMP)[1] is an important and ubiquitous second messenger in bacteria (*1*−*3*). The first demonstrated function for c-di-GMP was the discovery, by Benziman and colleagues, that c-di-GMP allosterically activates the cellulose synthase complex that produces the cellulosic raft covers of *Gluconacetobacter xylinus* (formerly *Acetobacter xylinum*) static cultures (*4*, *5*). Consistent with this initially observed role of c-di-GMP, most of the functions thus far discovered for the dinucleotide have related to bacterial cell-surface adhesiveness and biofilm formation (*6*−*10*). There is increasing interest in biofilms because they are known to protect bacteria from antibiotic exposure and to exacerbate some chronic infections in humans (*11*).

Since the pioneering work on *G. xylinus* and bioinformatics studies suggesting that the GGDEF/EAL-domain enzymes for c-di-GMP synthesis and degradation occur in many bacterial species, interest in this second messenger has been revived, and our understanding of it has grown (*3*, *7*, *12*−*15*). Nevertheless, fundamental questions remain unanswered about the c-di-GMP homeostatic mechanism. For example, what signals regulate the activities of the diguanylate cyclases (DGC) and c-di-GMP phosphodiesterases (PDE)? That such signals exist is indicated by the recognizable signaling domains in these proteins that accompany their enzymatic domains (*3*, *6*, *16*−*18*). Even so, relatively few studies have directly addressed the coupling of a signaling domain to a DGC or PDE activity (*19*−*21*). Another important question regards the *in vivo* targets of c-di-GMP. The range of c-di-GMP's influence was recently shown to include metabolite-binding regions in mRNAs that could be targeted for aborting specific transcripts (*22*). Though few protein targets have been identified for c-di-GMP, the example of the *G. xylinus* cellulose synthase represents an important precedent that this molecule can serve as an allosteric effector of target proteins (*4*). Additional proteins known to bind c-di-GMP include a putative c-di-GMP receptor and several DGCs that are allosterically inhibited by their cyclic nucleotide product (*21*, *23*, *24*). We have proposed that c-di-GMP acts via a direct activation or inhibition of a target molecule, rather than a change in the expression levels of the target, to govern adaptations that are too transient to be mediated by new gene expression (*6*, *25*).

[†]This work was supported by National Science Foundation Grant 620531 and Welch Foundation Grant I-1575 (to M.-A.G.-G.) and by National Science Foundation Grant MCB0446431 and U.S. Army Telemedicine and Advanced Technology Research Center Award W81XWH0520013 (to M.A.).

*Corresponding author. E-mail: Marie-Alda.Gilles-Gonzalez@UTSouthwestern.edu. Tel: 214-648-9438. Fax: 214-648-8856.

[1]Abbreviations: *Bpe* GReg, *Bordetella pertussis* globin-coupled regulator; c-di-GMP, 3′−5′ cyclic diguanylic acid (also cyclic di-GMP); DGC, diguanylate cyclase; DosC, *Escherichia coli* direct oxygen-sensing cyclase (referred to in other places as YddV or YhcK); $DosC_H$, DosC truncation containing only heme domain residues 2−160; DosP, *E. coli* direct oxygen-sensing phosphodiesterase (previously named *Ec* Dos); $DosP_H$, DosP truncation containing only heme domain residues 1−147; $FixL_H$, a truncation of *Sinorhizobium meliloti* FixL containing only heme domain residues 119−266; GGDEF and EAL, signature sequences found in diguanylate cyclases and c-di-GMP phosphodiesterases; HemAT-*Bs*, HemAT from *Bacillus subtilis*; *malE*, the gene encoding the *E. coli* maltose-binding protein; MBP, *E. coli* maltose-binding protein; PDE, c-di-GMP phosphodiesterase; *Gx* PDE-A1, *Gluconacetobacter xylinus* phosphodiesterase A1; SW Mb, sperm whale myoglobin. The alphanumeric code (e.g., E7) refers to the positions of amino acids in helices and turns of globins.

 Published on Web 09/18/2009

The numbers of GGDEF/EAL proteins encoded by bacteria pose yet another puzzle: why are so many of these proteins needed in some species if GGDEF domains reliably manifest a DGC activity and EAL domains a c-di-GMP-dedicated PDE activity (*18*, *26*, *27*)? The *Escherichia coli K12* genome, for example, encodes 12 proteins with a GGDEF domain, 10 with an EAL, and 7 with both GGDEF and EAL (*28*, *29*). By contrast to this panoply of c-di-GMP-dedicated enzymes, *E. coli* possesses a single adenylate cyclase and a single cAMP phosphodiesterase (*30*, *31*). Nevertheless, in several instances, a phenotypic change demonstrably results in a bacterium from the deletion of a single DGC or PDE (*21*, *32*−*34*). Why should this be so, if several other enzymes in the same cell can, in principle, complement this deficiency? For the GGDEF- and EAL-domain proteins, the genetic data have, on the whole, been inconsistent with a model where a freely diffusible intracellular pool of c-di-GMP regulates the adaptive responses. We propose instead that the observations favor a model where a specific DGC and PDE determine the availability of c-di-GMP to a precise target.

The presence of c-di-GMP at a specific site would in turn be governed by the physiological state of an organism and its environment. In such a scheme, the response of a DGC or PDE to physiological signal would be paramount. Oxygen appears to be a very important signal ligand for regulating DGCs and PDEs. Regulation by O_2 was first demonstrated for *G. xylinus* PDE-A1, the main *G. xylinus* enzyme that turns off cellulose synthesis (*19*). Shortly thereafter, an *E. coli* PDE highly homologous to *G. xylinus* PDE-A1 was identified and named *Ec* Dos (*E. coli* direct oxygen sensor) in anticipation of an O_2-regulated phosphodiesterase activity (*25*). More recently, Alam, Gilles-Gonzalez, and their colleagues found a diguanylate cyclase, *Bpe* GReg, in the whooping cough pathogen *Bordetella pertussis* and demonstrated that this enzyme is involved in biofilm production and subject to O_2 regulation (*21*). Altogether, these findings point to an important and intimate connection between O_2 and c-di-GMP metabolism.

Here we describe a heme-containing *E. coli* DGC, which we are naming *Ec* DosC (*E. coli* direct oxygen sensing cyclase). This protein had heretofore not been purified; however, it has long been noted to possess a GGDEF domain unaccompanied by an EAL, and the gene (variously called *yddV*, *yhcK*, and *Ec greg*) had for this reason been exploited for *in vivo* complementation experiments (*2*, *26*, *35*). *Ec* DosC closely resembles the *B. pertussis* cyclase *Bpe* GReg in sequence, but the two proteins differ in at least one important respect: *Ec dosC* is expressed jointly with *Ec dos* in a translationally coupled operon, whereas *Bpe greg* is expressed singly from a genome that possesses no *Ec dos* homologue. We propose here that the "*dos*" gene name be modified to "*dosP*", for direct oxygen sensing phosphodiesterase, to acknowledge this protein's enzymatic activity in addition to its sensing function and to distinguish it from other potential O_2 sensors in *E. coli*. Our study demonstrates that the expression of the *E. coli dosCP* operon yields a functional complex of DosC and DosP. In addition, the studies reveal a DosP O_2 dose response that is consistent with the detection of slowed cell growth.

MATERIALS AND METHODS

Genetic Manipulations. The designs of oligonucleotide primers for amplifying regions of the *dosCP* operon were based on the *E. coli* genome sequence published by Blattner and colleagues (*36*). *E. coli* genomic DNA served as the template in polymerase chain reactions (PCR). The PCR primers appended a *Nsi*I or *Nde*I restriction site to the 5′ end and a *Hin*dIII or *Not*I site to the 3′ end of each amplified DNA. The amplified products with *dosCP* and $dosC_H$ (codons 2−160) were cloned as *Nsi*I−*Not*I fragments into an *E. coli pUC19*-based expression vector such that the final plasmids conferred ampicillin resistance and *tac*-promoter control of the recombinant genes. The *E. coli malE* gene was fused to the 5′ end of *dosC* by cloning the *dosCP*-coding sequence as a *Nsi*I−*Not*I fragment into the *E. coli* vector pMAL-c2e (New England Biolabs), where *Nsi*I and *Not*I restriction sites were engineered into the polylinker.

Gene Expression and Protein Purification. The *dosCP* operon was overexpressed in *E. coli* in a Bioflow 3000 4-L fermentor with continuous supplementation of LB and glucose. This fermentor features automatic control of temperature via electrical heating and circulation of chilled water so that any programmed temperature is reached within 2 min and maintained automatically within 0.1 °C. It was initially set to 37 °C. The pH was programmed for 7.5 and was automatically maintained within 0.2 unit of this value by precise additions of neat NH_4OH to neutralize bacterial catabolites. The O_2 electrode was calibrated by agitating the medium vigorously with air and setting that point as 100% air saturation once the electrode reading stabilized. The O_2 concentration was set to 4% O_2 (i.e., 20% of atmospheric O_2) and maintained by automatic adjustments of the agitation rate and the percentage of O_2 in a feed of air and pure O_2. When the cultures reached 30 g/L of wet cells, isopropyl β-D-1-thiogalactopyranoside (IPTG) was added to a final concentration of 1.0 mM, and the fermentor temperature was changed to 27 °C. The cells were harvested 20 h later. The $dosC_H$ region, encoding a sensory globin domain, and the *malE:dosC* fusion were expressed in shaker cultures of *E. coli*. The media initially consisted of LB with 200 μg/mL ampicillin and 0.2% (w/v) glucose. When the cultures reached $A_{600} \sim 0.5$, gene expression was induced with 1.0 mM IPTG, and the temperature was reduced to 27 °C. The cells were harvested 4−8 h postinduction.

All subsequent protein purification steps were at 4 °C, with monitoring of the proteins from their bright red color or absorption spectra (Cary 4000 UV−vis spectrophotometer; Varian). The *dosCP*-overexpressing cells were lysed by sonicating the harvested cell pellet in lysis buffer [50 mM Tris-HCl, pH 8.0, 150 mM NaCl, 5.0 mM dithiothreitol (DTT), 1.0 mM EDTA, 0.050 mg/mL lysozyme, and 0.17 mg/mL PMSF]. After 40 min of centrifugation at 70000 rpm, the cleared lysate was brought to 0.40 M $(NH_4)_2SO_4$ and loaded onto a phenyl-Sepharose fast-flow column (GE Healthcare) equilibrated with 0.40 M $(NH_4)_2SO_4$ in FS buffer (50 mM Tris-HCl, 150 mM NaCl, 5.0 mM DTT, 1.0 mM EDTA, pH 8.0). The column was washed sequentially with FS buffer containing 0.40, 0.20, and 0.10 M $(NH_4)_2SO_4$ prior to elution of the bound DosC−DosP complex with FS buffer without $(NH_4)_2SO_4$. The recovered DosC−DosP complex, easily identified by its color, was loaded onto a 1 m × 25 mm Superdex S200 column (GE Healthcare) preequilibrated with 50 mM Tris-HCl, 50 mM NaCl, and 5.0% (v/v) glycerol, pH 8.0. The collected fractions were analyzed for their purity and protein contents from their spectra, from Bradford protein assays (Bio-Rad), and from Coomassie-stained SDS−PAGE gels (*37*).

Cells overproducing $DosC_H$ were sonicated in the same lysis buffer described above, except for replacement of DTT with β-mercaptoethanol (10 mM). After 40 min of centrifugation at

70000 rpm, the cleared lysate was brought to 1.2 M $(NH_4)_2SO_4$ and centrifuged at 12000 rpm for 15 min. The pellet was discarded, and the supernatant was slowly brought to 2.4 M $(NH_4)_2SO_4$. After 15 min of centrifugation at 12000 rpm, the protein pellets were stored at −80 °C. Later the protein pellets were resuspended in 2 volumes of 20 mM Tris-HCl and 10 mM β-mercaptoethanol, pH 8.0, and a small fraction of undissolved materials was removed by 15 min of centrifugation at 12000 rpm. The supernatant was desalted through a Sephadex G25 column preequilibrated in 20 mM Tris-HCl and 10 mM β-mercaptoethanol, pH 8.0, and then applied to a DEAE-Sepharose 10 cm (height) × 3 cm (diameter) column preequilibrated with the same buffer. After thorough washing of the column with the loading buffer, the $DosC_H$ was slowly eluted from buffer supplemented with 150 mM NaCl. The eluted $DosC_H$ was concentrated, purified to homogeneity by gel-filtration chromatography (Superdex S200, 1 m × 25 mm; GE Healthcare), and stored at −80 °C.

For MBP-DosC, the harvested cells (~24 g) were resuspended in 40 mL of lysis buffer [50 mM Tris-HCl, pH 8.0, 150 mM NaCl, 5 mM $MgCl_2$, 1 mM DTT, 5% (v/v) glycerol] and centrifuged at 5000 rpm for 15 min, and the resulting cell pellets were frozen initially on dry ice and then overnight at −20 °C. Twelve grams of frozen cells was resuspended in 35 mL of lysis buffer supplemented with 42 mg of lysozyme and 7 mg of PMSF and incubated on ice for 20 min. The cells were then completely disrupted by sonication and centrifuged at 70000 rpm for 35 min, and the supernatant was applied directly onto an amylose-resin matrix [9 cm (height) × 2 cm (diameter); New England Biolabs] preequilibrated with lysis buffer. After extensive washing with wash buffer (50 mM Tris-HCl, pH 8.0, 200 mM NaCl, 1 mM EDTA, 1 mM DTT), the bound MBP-DosC was eluted with wash buffer containing 10 mM maltose. Glycerol was added to the eluted MBP-DosC to a final concentration of 5% (v/v), and the purified protein was frozen with liquid N_2 and stored at −80 °C.

Absorption Spectra, Ligand Binding, and Autoxidation. Unless otherwise noted, all determinations of UV−vis absorption and ligand binding were for 2−5 μM protein in 0.10 M sodium phosphate, pH 7.5 at 25 °C. Absorption spectra were monitored with a Cary 4000 UV−vis spectrophotometer (Varian). Laser-flash photolysis and stopped-flow measurements were made with an LKS.60 laser kinetic spectrometer fitted with a PiStar stopped-flow drive unit (Applied Photophysics, Leatherhead U.K.). For sample excitation, the LKS.60 spectrometer was coupled to a Quantel Brilliant B Nd:YAG laser with second-harmonic generation. Ligand-binding kinetics were followed at a wavelength of maximum difference between the starting and final species. Each association rate constant was calculated from a linear plot of k_{obsd} versus ligand concentration including at least four ligand concentrations.

Binding of O_2, CO, and NO was measured for the ferrous forms of the heme proteins, and binding of imidazole and cyanide was measured for their ferric forms. Association rates for O_2 (80−1280 μM) and NO (30−240 μM) were measured by laser-flash photolysis at two wavelengths (412−417 and 433−435 nm). Association rates for CO (30−960 μM) were measured by both stopped-flow and laser-flash photolysis at two wavelengths (419 and 433−435 nm). Association rates for imidazole (0.25−4.0 mM) and cyanide (12.5−50 mM) were measured by stopped-flow at 390 and 420 nm, respectively. The O_2 dissociation rate constant was measured by stopped flow at both 412 and 433−435 nm by mixing oxy protein in 50−256 μM free O_2 with a solution of 2.0 mM sodium dithionite. The CO dissociation rate constant was measured by ligand replacement in the stopped flow at 421 nm by mixing carbonmonoxy protein in 10−30 μM free CO with a 1.0−2.0 mM solution of NO. The cyanide dissociation rate constant was measured as follows: met-$DosC_H$ was equilibrated with 1.0 mM KCN and passed through a desalting column (Biospin; Bio-Rad) preequilibrated with 0.10 M sodium phosphate and 0.20 M imidazole, pH 7.5, and whole absorption spectra were recorded for the transition from cyanomet to imidazolemet $DosC_H$. The spectra were deconvoluted into cyanomet and imidazolemet components by multiple linear regression, and the rates were calculated from the change in the fraction of imidazolemet-$DosC_H$ over time.

The equilibrium dissociation constants for binding of O_2 and CO were measured directly by mixing the deoxy protein with 1.0−1280 μM O_2 or 1.0−960 μM CO dissolved in buffer (0.10 M sodium phosphate, pH 7.5). Linear combinations of whole basis spectra for the deoxy, oxy, and carbonmonoxy states of the protein were used to determine its saturation at varying O_2 and CO concentrations. K_d and Hill constant were calculated by fitting the saturation versus ligand concentration curve ($R^2 > 0.99$) to the Hill equation in Excel.

Diguanylate Cyclase Assays. Assays of diguanylate cyclase activity were done for 1−5 μM DosC in 20 mM sodium phosphate, pH 7.5, 10 mM $MgCl_2$, and 2.0 mM DTT at 30 °C. To start the reactions, GTP (α-^{32}P-labeled; Perkin-Elmer) was added to 500 μM. At the appropriate times, an aliquot of the reaction mixture was removed and added to an equal volume of 0.10 M EDTA, pH 8.0. Stopped time points were heated at 95 °C for 5 min and centrifuged, and 1−2 μL of the supernatant was spotted onto polyethyleneimine−cellulose thin-layer chromatography plates (PEI-TLC; Merck KGaA, Darmstadt, Germany) and developed in a 1.5:1.0 mixture of KH_2PO_4 (1.5 M, pH 3.6):$(NH_4)_2SO_4$ (4.0 M, pH 3.6). Under these conditions, GTP migrates with R_f = 0.58, pGpG with R_f = 0.34, and c-di-GMP with R_f = 0.18. The dried TLC plates were imaged with a storage phosphor screen (Kodak K-HD) and a Personal Molecular Imager FX phosphorimager (Bio-Rad) and quantified with Quantity One software version 4.4.0 (Bio-Rad).

Cyclic di-GMP Production and Purification. Radioactive and nonradioactive c-di-GMPs were synthesized enzymatically from [α-^{32}P]GTP (Perkin-Elmer) or GTP (Roche) using *Bpe* GReg (*21*). Overnight reactions were heated at 95 °C for 10 min and centrifuged to remove the precipitated *Bpe* GReg, and the supernatant was loaded onto a Sep-Pak C18 cartridge (Waters, Milford, MA). The column was washed with 3 volumes of 0.15 M KH_2PO_4 and eluted with acetonitrile. The solvent from the eluted c-di-GMP was evaporated by drying under a stream of N_2. The crystalline c-di-GMP was resuspended in 10 mM Tris-HCl, pH 8.0, and stored at −20 °C. The c-di-GMP purity was determined by HPLC, and the concentration was calculated from the 253 nm absorption (ε_{253} = 23700 M^{-1} cm^{-1}).

Phosphodiesterase Assays. Deoxy-DosP was prepared by reducing the protein with DTT in an anaerobic glovebag (Coy, Grasslake, MI). Oxy-DosP was prepared by bubbling air into samples of deoxy-DosP. Assays of phosphodiesterase activity were done for 0.20−1.0 μM DosP in 20 mM sodium phosphate, 10 mM $MgCl_2$, and 2 mM DTT, pH 7.5 at 30 °C. To start the reactions, c-di-GMP (unlabeled or ^{32}P-labeled) was added to a final concentration 10−100 μM. At the appropriate times, an aliquot of the reaction mixture was removed and added to an equal volume of 0.10 M EDTA, pH 8.0. Stopped time points were

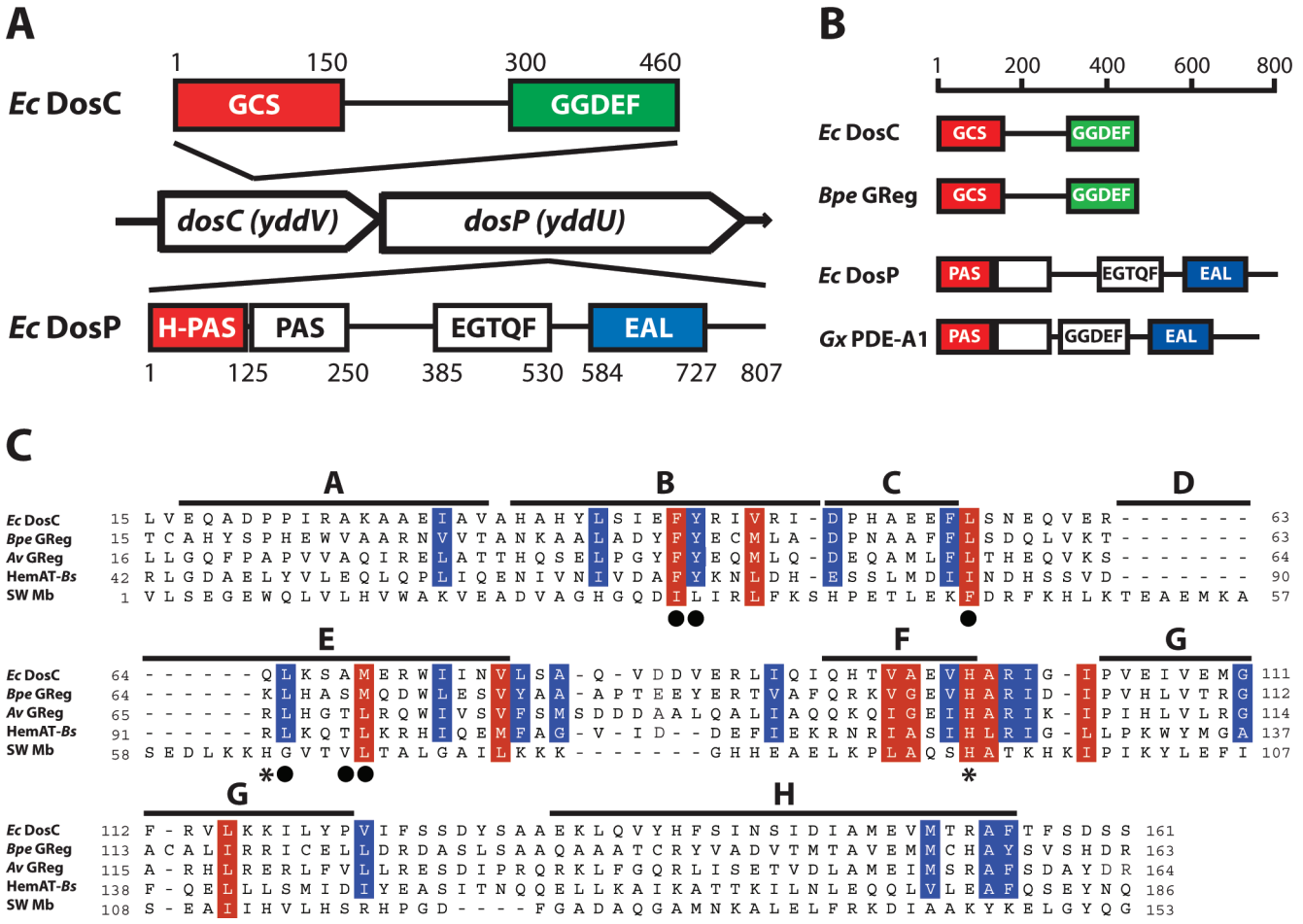

FIGURE 1: Two heme-based sensors encoded by an operon for c-di-GMP homeostasis. (A) Genetic organization of the *E. coli dosCP* operon and domain organizations of the corresponding proteins. The first gene in the operon was provisionally named *yddV* or *yhcK*; we renamed it *dosC* for direct oxygen-sensing cyclase. The second gene was provisionally named *yddU* and later named *dos*; we are proposing here that the name be amended to *dosP* for direct oxygen-sensing phosphodiesterase. (B) Domain organizations of O_2-sensing enzymes for c-di-GMP homeostasis. The GGDEF enzymes couple a diguanylate cyclase to an N-terminal modified globin domain. The EAL enzymes couple a c-di-GMP phosphodiesterase to an N-terminal heme-binding PAS domain. (C) Amino acid sequence alignment of the sensory region of DosC with that of the known globin-coupled sensor *Bpe* GReg, the known heme-binding protein *Av* GReg, and structural alignments of HemAT-*Bs* with sperm whale myoglobin (SW Mb) (*21*, *61*). The lines above the sequences indicate the A- through H-helices of SW Mb. The residues highlighted in red are conserved in the sensory globins and SW Mb; those highlighted in blue are similar in the GCSs but different from corresponding positions in SW Mb. The asterisks denote the SW Mb proximal (F8) histidine of heme attachment and distal (E7) histidine; the filled circles indicate HemAT-*Bs* residues lining the ligand-binding heme distal pocket (*39*).

heated at 95 °C for 5 min and centrifuged to remove the precipitated DosP. Radioactive samples were processed, imaged, and quantified as described above for the DGC assays. Non-radioactive samples (10 μL) were loaded onto an Adsorbosphere Nucleotide-Nucleoside reversed-phase HPLC column (Alltech, 250 × 4.6 mm) equipped with an Adsorbosphere Nucleotide-Nucleoside guard column (Alltech/Grace, 7.5 × 4.6 mm). The mobile phase consisted of (A) 0.15 M NaH_2PO_4, pH 5.2, and (B) 40% (v/v) acetonitrile balanced with 0.15 M NaH_2PO_4, pH 5.2. A linear gradient from 0% to 35% buffer B for 10 min at 1 mL/min was used to separate the pGpG product from the c-di-GMP substrate.

RESULTS

The E. coli dosCP Operon Encodes Two Sensory Heme Proteins. The *dosC-dosP* region of the *E. coli* genome, previously designated *yddV-yddU* or *yhcK-yddU,* constitutes a two-gene operon where both of the genes encode heme proteins for c-di-GMP homeostasis (Figure 1). The promoter for this operon resides upstream of *dosC*, and only the *dosC* stop codon separates this gene from the start of *dosP* (*35*). This genetic organization indicated coupling, not only of *dosCP* transcription but also of DosC and DosP translation. We therefore supposed that, like other bacterial genes that are thus organized, e.g., many histidine−protein kinase and response−regulator couples, the products of the *dosCP* operon might jointly function. *E. coli* DosP (formerly called Dos or *Ec*Dos) is relatively well studied and is known to join a heme-binding PAS domain to a c-di-GMP phosphodiesterase region (*25*, *38*). By contrast, *E. coli* DosC had never been purified. This protein had, however, been noted to contain a C-terminal GGDEF domain without an accompanying EAL, and the overexpression of its gene had been exploited to complement deletions of GGDEF-domain proteins from several heterologous hosts (*2*, *26*, *35*).

In Figure 1, the DosC N-terminal domain sequence was compared to the sequences of other sensory globins, some of which are of known structure. This comparison showed DosC to be more closely related to the sensory globins (47% sequence similarity and 18% identity to HemAT-*Bs*) than to mammalian Mb. Many globins from organisms as diverse as vertebrates,

insects, and plants share a general structural fold that allows certain features to be compared. Sensory globins, which are considered more ancient, do not share all of these features. For example, the entire D-helix and the first half of the E-helix, including the typical distal (E7) histidine, are absent from HemAT-*Bs*; we expect that this is also true for DosC (*17*, *39*, *40*). The homology between DosC and mammalian globins is very low. The main globin residues conserved in DosC were the F8-histidine residue of heme attachment and the C2-proline (H98 and P50, respectively). In the alignment, the closest DosC relative was *Bpe* GReg (55% similarity and 34% identity overall): a proven globin-coupled sensor with O_2-regulated DGC activity (*21*).

To determine if DosC binds heme in its N-terminal region, we examined two versions of this protein for the presence of heme: the $DosC_H$ fragment, representing only the sensory globin domain, and a MBP-DosC fusion with the full-length protein (Figure 2A). Size-exclusion chromatography showed the $DosC_H$ construct to be dimeric, and pyridine hemochromogen assays determined both $DosC_H$ and MBP-DosC to contain one heme per monomer (not shown) (*41*). Absorption spectra of DosC further confirmed its heme protein nature and the capacity of its ferrous state to bind ligands such as O_2 and CO and the ferric state to bind ligands such as CN^- and imidazole (Figure 2B).

DosC Presents an Accessible but Apolar Binding Site to O_2 and Other Heme Ligands. The met form of DosC (Fe^{III}) showed an absorption spectrum typical of heme with a five-coordinate high-spin iron atom. Specifically, the spectrum showed a Soret absorption band around 391 nm, together with a broad and less intense band around 500 nm, and a smaller peak around 650 nm (Figure 2B). Spectra of this sort indicate that water or hydroxide do not coordinate to the heme iron in the ferric state. In two well-established cases where met spectra similar to that of met-DosC were observed, this was explained by the inability of distal pocket residues to accept a hydrogen bond from bound water or hydroxide (*42*−*45*). Additional evidence for an apolar heme pocket comes from the relatively slow kinetics of cyanide binding to met-DosC (Table 1). Cyanide enters the heme pocket exclusively as the neutral protonated HCN species, both because this species comprises >99% of the cyanide at neutral pH and because the charged CN^- species is effectively excluded from the hydrophobic heme pocket (as even the most "polar" ligand-binding heme pocket is far more hydrophobic than aqueous solution). Since HCN is not a heme ligand, the HCN molecule must transfer its proton to a distal pocket residue before it can bind to heme iron. The kinetics of cyanide binding in all heme proteins for which this reaction has been studied is limited by the rate of this deprotonation of neutral HCN inside the heme pocket; for DosC these kinetics suggest that a readily ionizable residue is not near to the bound ligand (*46*). Consistent with this hypothesis, the alignment in Figure 1C suggests that the DosC heme distal pocket is lined with residues F42, Y43, L56, L65, A68, and M69. Compared to SW Mb, the DosC heme iron bound cyanide 100 times more slowly, yet it bound imidazole 30 times more rapidly. Since the factor limiting the kinetics of binding for ligands as bulky as imidazole is usually steric accessibility, we may conclude that the DosC pocket is much less sterically constrained than that of SW Mb (Table 1) (*47*).

DosC binds O_2 about 30-fold less tightly than the homologous *Bpe* GReg (Table 2). Compared to *Bpe* GReg, the DosC association rate constant for binding of O_2 was 4-fold lower, whereas the dissociation rate constant was 8-fold higher (Table 2). The MBP-DosC and $DosC_H$ constructs showed a similar O_2 affinity ($K_d \sim 10-20\ \mu M$) (Figure 3, Table 2). Likewise, the two

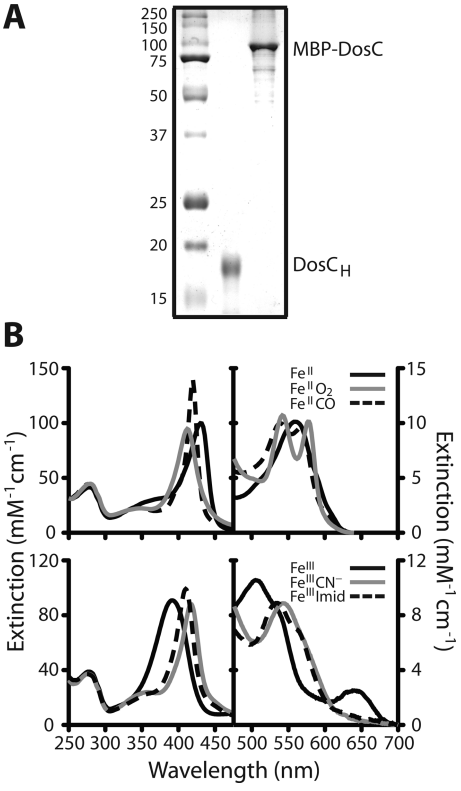

FIGURE 2: *E. coli* DosC contains a sensory globin domain. (A) Coomassie-stained SDS−PAGE showing two soluble constructs of *E. coli* DosC: the $DosC_H$ and MBP-DosC proteins. (B) Absorption spectra. The top panel show ferrous species: deoxy (Fe^{II}, black), oxy ($Fe^{II}O_2$, gray), and carbonmonoxy ($Fe^{II}CO$, broken line). The bottom panel shows ferric species: met (Fe^{III}, black), cyanomet ($Fe^{III}CN^-$, gray), and imidazolemet (Fe^{III}Imid, broken line).

Table 1: Ligand-Binding and Autoxidation Parameters of Selected Heme Proteins[a]

	CN^-			imidazole			
	k_{on} ($mM^{-1}\ s^{-1}$)	k_{off} (s^{-1})	K_d (μM)	k_{on} ($mM^{-1}\ s^{-1}$)	K_d (mM)	Met λ max (nm)	k_{ox} (h^{-1})
$DosC_H$[b]	0.0028	0.000017	6.1[c]	5.0	0.075[d]	391	2.4
$FixL_H$	0.027	0.0001	4.6	50	2	395	2.3
SW Mb	0.32	0.0004	1.3	0.16	22	409	0.06

[a]Heme proteins were selected to demonstrate a wide range of ferric ligand-binding parameters. [b]This work. [c]Calculated from k_{off} and k_{on}. [d]Measured by direct titration. Measurements on *Sinorhizobium meliloti* $FixL_H$ are from Gilles-Gonzalez et al. (*57*) and Winkler et al. (*58*). Measurements on SW Mb are from Quillin et al. (*59*), Dou et al. (*46*), Mansy et al. (*47*), and Brantley et al. (*60*).

Table 2: Ligand-Binding Parameters of Oxygen-Regulated Diguanylate Cyclases and Phosphodiesterases

	O_2			CO			NO
	k_{on} (μM^{-1} s^{-1})	k_{off} (s^{-1})	K_d (μM)[f]	k_{on} (μM^{-1} s^{-1})	k_{off} (s^{-1})	K_d (μM)[f]	k_{on} (μM^{-1} s^{-1})
MBP-DosC[a]	1.8	36	21	0.13	0.13	0.98	
$DosC_H$[a]	3.2	18	9.7	0.13	0.080	0.64	7.9
Bpe GReg [b]	7.1	4.5	0.63*	1.0	0.57	0.057*	16
				0.13		0.44*	
DosP[a]	0.0092[g]	0.82	74	0.0029[g]	0.023	8.0	
$DosP_H$[c]	0.0026	0.034[h]	13	0.011	0.011[h]	10	0.0018
PDE-A1 [d]	6.6	77	12*	0.21	0.58	0.28*	
DosP [e]	0.0019	0.64	340*	0.00081	0.0025	3.1*	
$DosP_H$[e]	0.031	0.61	20*	0.0078	0.0045	0.58*	

[a]This work. Measurements were at pH 7.5 and 25 °C. [b]Wan et al. (*21*). Measurements were at pH 7.5 and 25 °C. [c]Delgado-Nixon et al. (*25*). Measurements were at pH 7.0 and 20 °C. [d]Chang et al. (*19*). Measurements were at pH 8.5 and 25 °C. [e]Taguchi et al. (*51*). PDE-A1 is from *G. xylinus* (formerly *A. xylinum*). Measurements were at pH 8.0 and 25 °C. [f]K_d values were measured by direct titration except where indicated by an asterisk, where they were calculated from k_{off} and k_{on}. [g]Calculated from k_{off} and K_d. [h]Calculated from k_{on} and K_d.

constructs showed a similar CO affinity ($K_d \sim 1$ μM) (Table 2). The kinetics for binding of ligands were also alike for the constructs. Overall, DosC is better suited to respond to O_2 in the microaerobic regime (10 s of micromolar O_2) (Figure 3). In this respect, DosC differs significantly from *Bpe* GReg, which is set to respond to micromolar O_2.

Ligand Binding by DosP. We directly measured the ligand affinity of DosP by titration with ligands. From this study, we determined the equilibrium dissociation constant for O_2 binding to be 74 μM and that for CO binding to be 8.0 μM (Table 2; also see Figure 5). In addition, we discovered a cooperative binding of ligands, with a Hill coefficient n of 1.5 for O_2 and 1.2 for CO (Figure 5A,C). These data disagree with a K_d value of 340 μM estimated from kinetics (*51*). Such a low affinity implies less than 50% saturation with O_2 in air and is inconsistent with our direct titration (Figure 5A) (*51*).

DosP and its isolated heme-binding domain $DosP_H$ show a similar hexacoordination of their unliganded heme iron atom. This has been reported as a histidine−Fe−methionine coordination (*25*, *48*−*50*). However, $DosP_H$ differs from DosP in some important respects. Binding of ligands to $DosP_H$ is noncooperative (n of 1.0 for O_2 and CO); the affinity for O_2 (K_d of 13 μM) is 6-fold higher than that of DosP, and this increased affinity is associated with a slower O_2 off-rate constant (Table 2) (*25*).

Ligand−Dose Response of the DosP c-di-GMP Phosphodiesterase. Figure 4 shows representative HPLC traces for the conversion of c-di-GMP (100 μM) to the linear pGpG by deoxy-DosP versus oxy-DosP (1 μM enzyme). Saturation of DosP with O_2 enhanced the phosphodiesterase activity 17-fold over the deoxy state (50 min^{-1} compared to 3 min^{-1}). We estimate a K_M value of about 4 μM with respect to c-di-GMP for the oxy state, from numeric fitting of the end of the reaction time course when substrate concentration is low. Both the oxy- and deoxy-DosP phosphodiesterase reactions went to completion, although the latter required about 30 min (Figure 4). We tested whether the activity of DosP might be allosterically enhanced by GTP, as noted for another c-di-GMP phosphodiesterase, but we saw no effect of GTP on the reaction rate (*52*). Carbon monoxide saturation enhanced the activity to the same extent as O_2 saturation. This indicates that ligand polarization upon binding to heme does not contribute significantly to the regulatory mechanism as it does in FixL, for which O_2 is an inhibitor and CO a weak antagonist (*53*).

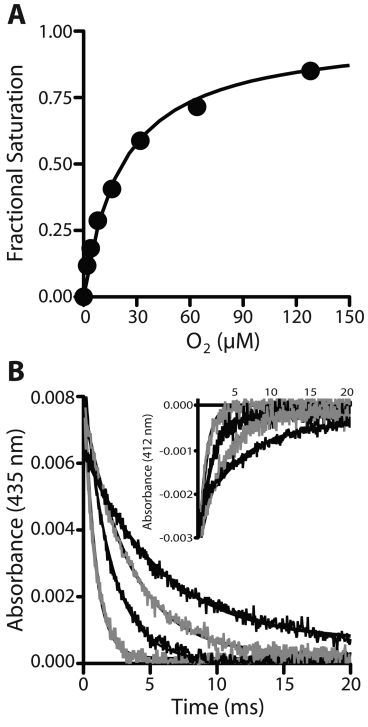

FIGURE 3: Binding of O_2 to *E. coli* DosC. (A) Determination of the DosC affinity for O_2 at pH 7.5 and 25 °C. A K_d value of 21 μM was determined by directly titrating MBP-DosC with 0−1280 μM O_2, deconvoluting the deoxy and oxy fractions in the absorption spectra, and fitting the data to a hyperbolic equation for single binding using least-squares analysis. Details are under Materials and Methods. (B) Representative kinetic traces showing the rates of O_2 association to MBP-DosC at pH 7.5 and 25 °C. The main panel shows the accelerating rates as the DosC binds 80, 160, 320, and 640 μM O_2, as monitored at 435 nm from the disappearance of the deoxy state; the inset shows the same process monitored at 412 nm from the appearance of the oxy state. Rates were measured by laser-flash photolysis, as described under Materials and Methods. Similar results were obtained with $DosC_H$.

We found the response of DosP to ligand saturation to be highly nonlinear and skewed toward high saturation (Figure 5). There was hardly any effect of O_2 until the protein became 50% saturated. In particular, over 80% of the 17-fold enhancement of the activity by ligand occurred in the second half of the heme titration (O_2 > 75 μM). In other words, a drop in the O_2 saturation of only 20% from full saturation resulted in a loss of

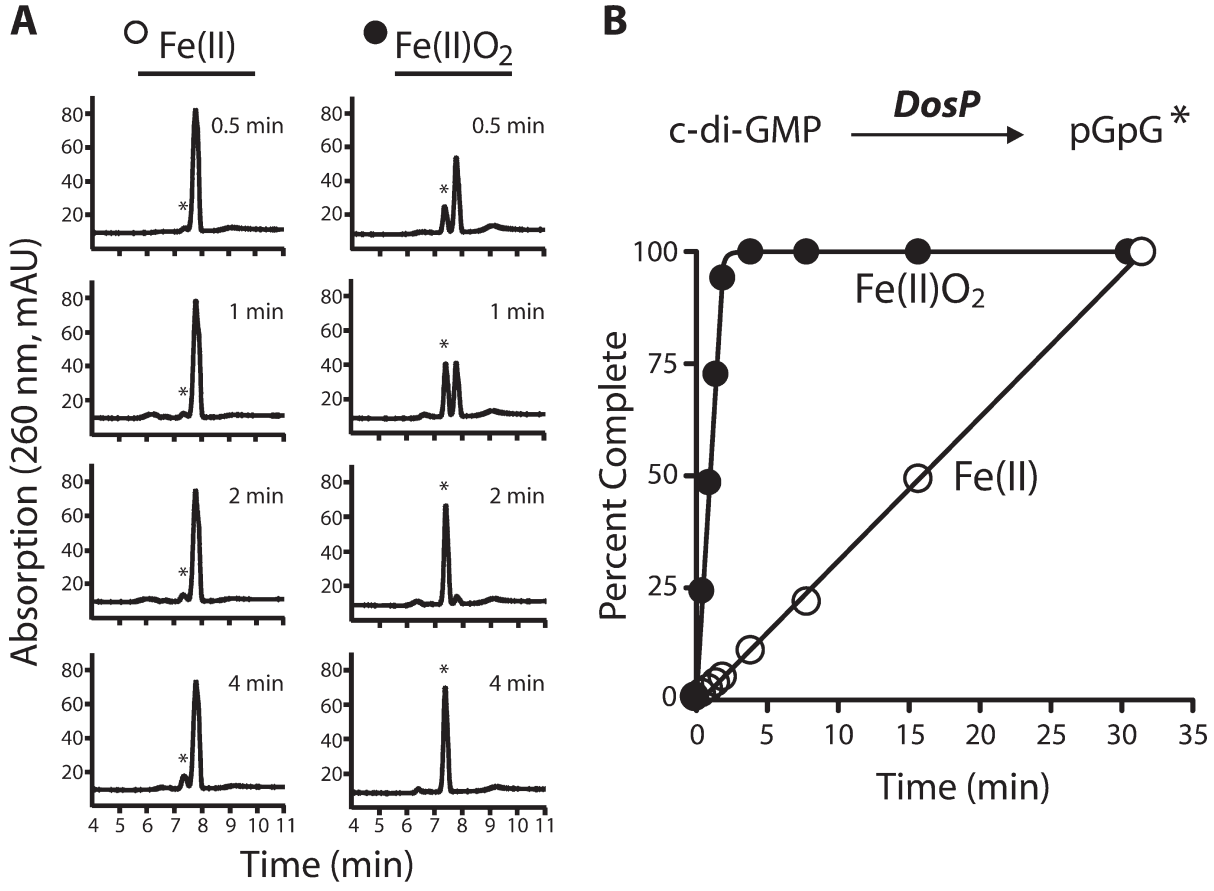

FIGURE 4: Oxygen switching of the c-di-GMP-specific phosphodiesterase in *E. coli* DosP. (A) Ferrous DosP (1 μM) without ligand (Fe^{II} or deoxy, open circles) or saturated with O_2 ($Fe^{II}O_2$ or oxy, closed circles) was assayed for its ability to catalyze the conversion of c-di-GMP (100 μM) to the linear pGpG. Representative HPLC traces for stopped time points are shown. The c-di-GMP peak migrates at 7.8 min, and the pGpG peak (indicated by an asterisk) migrates at 7.4 min. (B) An analysis of the complete phosphodiesterase data shows that ligation with O_2 enhances the phosphodiesterase activity of DosP more than 16-fold (to 50 min^{-1}) over the activity of the unliganded protein (3 min^{-1}). For both the liganded and the unliganded protein, the reaction velocity is maintained, even in little remaining substrate, until the reaction reaches completion. Similar results were obtained from TLC and autoradiographic analyses of reactions supplied with [α-^{32}P]-c-di-GMP.

over half of the O_2 activation. DosP has been reported to be homotetrameric and, as such, can have zero, one, two, three, or four bound O_2 per DosP tetramer, with each species having a potentially different phosphodiesterase activity (*54*). The concentration of each species at any O_2 saturation is straightforward to determine from the known O_2 titration curve. Unfortunately, while it is very clear that multiple oxygenations are required for activation, no assignment of activities to each known concentration of liganded species accurately accounts for the observed dose response (Figure 5). The dimeric protein kinase FixL achieves a highly nonlinear response to O_2 concentrations via a lag time between O_2 dissociation and the completion of the activation process (*53*). Analogous "memory effects" in DosP could potentially result in ten different states, which might completely explain the DosP dose response but would be daunting to model. The dose response for CO was similar in shape to the O_2 response curve and can be fairly well approximated by assigning all activation to the tetraliganded species (Figure 5B,D). The DosP dose response, along with other physical limitations, fix the DosP activation in *E. coli* to a relatively narrow range of O_2 concentrations: 75−256 μM O_2 (i.e., 30−100% saturation with air). On the other hand, the range of CO (> 10 μM) required for activating DosP well exceeds the concentrations that an *E. coli* cell would naturally encounter.

Association of DosC with DosP. Despite the considerable experience we gained on diguanylate cyclases during our successful studies of *Bpe* GReg, our efforts in two laboratories to examine the independent cyclase activity of DosC were unsuccessful (*21*). We wondered whether the translational coupling of the *dosC* and *dosP* genes, which implied a coordinated production of the two sensors, might also indicate their physical association. To test this idea, we moderately overexpressed the *dosCP* operon in *E. coli*. Two different purification schemes resulted in copurification of the proteins. The first purification was a two-step procedure involving hydrophobic interaction and size-exclusion chromatographies (phenyl-Sepharose and then S200 gel filtration) on a lysate of *E. coli* expressing an intact *dosCP* operon. The recovered sample contained two prominent protein bands, as analyzed by SDS−PAGE, and these were of the expected molecular masses for DosC (53 kDa) and DosP (91 kDa) (Figure 6A). Mass spectrometric (Maldi-MS) analysis of the sample showed two major molecular mass peaks at 53.5 and 90.5 kDa. Importantly, the purified protein sample contained both diguanylate cyclase and c-di-GMP-specific phosphodiesterase activities (Figure 6B,C). Another purification scheme involved the affinity chromatography of a lysate of *E. coli* expressing the operon as a *malE-dosC* fusion together with *dosP*. This resulted in comigration of the proteins (data not shown). We therefore concluded that the expression of the dosCP operon yields a complex of MBP-DosC and DosP.

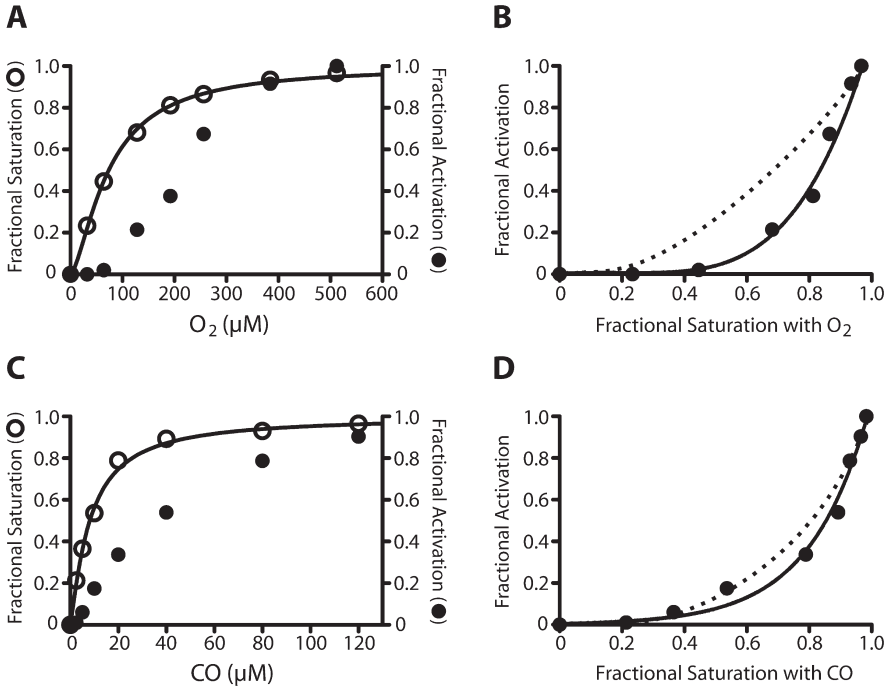

FIGURE 5: O_2 and CO dose responses of the *E. coli* DosP c-di-GMP phosphodiesterase. (A) Comparison of the effects of increasing O_2 concentrations (0−512 μM) on the fractional saturation of the DosP heme (open circles) and on the fractional activation of the DosP phosphodiesterase (closed circles). (B) Data from part A, recast as the fractional activations resulting from fractionally saturating the DosP heme with O_2. Dotted line: fit of the data to a model incorporating positive cooperativity within a tetramer. (C) Comparison of the effects of increasing CO concentrations (0−120 μM) on the fractional saturation of the DosP heme (open circles) and on the fractional activation of the DosP phosphodiesterase (closed circles). (D) Data from part C, recast as the fractional activations resulting from fractionally saturating the DosP heme with CO. Dotted line: fit of the data to a model incorporating positive cooperativity within a tetramer.

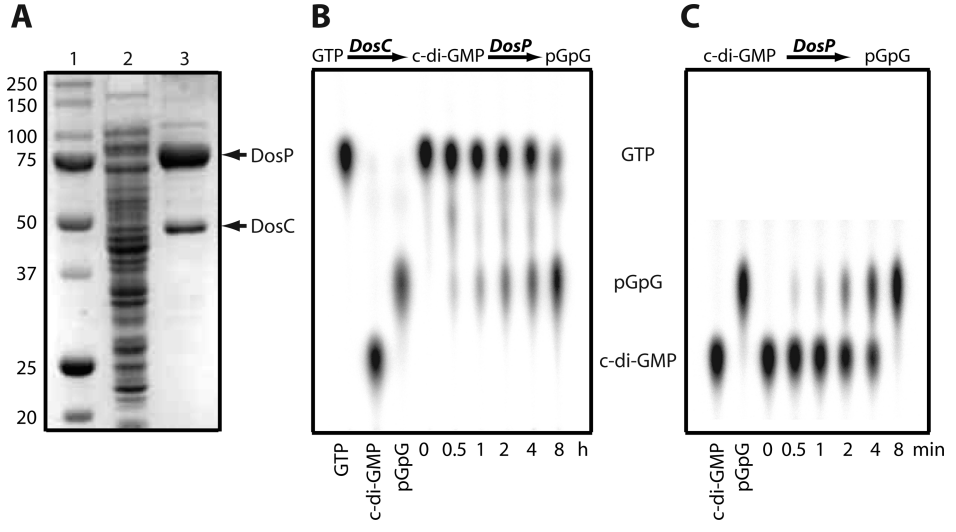

FIGURE 6: The DosC and DosP proteins copurify from *E. coli*. (A) Purification of DosC and DosP from *E. coli* moderately overexpressing the wild-type *dosCP* operon. A crude cell lysate (lane 2) from the dosCP-expressing cells is compared by Coomassie-stained SDS−PAGE to molecular weight markers (lane 1) and the copurified proteins (lane 3) after phenyl-Sepharose and gel-filtration chromatographies. (B) Presence of diguanylate cyclase activity in the DosC−DosP complex, as measured from the conversion of an [α-^{32}P]GTP substrate to ^{32}P-labeled linear pGpG, in a coupled assay. (C) Presence of c-di-GMP-specific phosphodiesterase activity in the DosC−DosP complex, as measured from the conversion of a ^{32}P-labeled c-di-GMP substrate to linear pGpG.

DISCUSSION

Cyclic di-GMP homeostasis is clearly important to bacteria for a variety of reasons, perhaps the most critical one being that this molecule typically regulates broad changes in lifestyle. Some of these changes include transitions from a motile to a sessile state that might involve interactions with a eukaryotic host. We and others have noted that the GGDEF and EAL domains which synthesize and degrade c-di-GMP, respectively, are often found associated with signaling domains (*3*, *6*, *16*−*18*). We have also shown that O_2 regulates the PDE-A1 protein involved in *G. xylinus* cellulose production and likewise regulates the *Bpe* GReg protein involved in *B. pertussis* biofilm production (*19*, *21*). Apart from representing the first demonstrations of signal regulation of enzymes for c-di-GMP metabolism, these results underline the fact that O_2 plays an extremely important role in

c-di-GMP homeostasis. This notion is given yet more weight by the work described in the current paper, i.e., the demonstration that *E. coli* possesses a two-gene operon, *dosCP*, that produces a complex dedicated to the coordination of c-di-GMP production and breakdown by O_2.

The *dosCP* operon is under the control of the general stress response and stationary phase sigma factor σ^S (RpoS), and as such the expression of this operon is induced by the entry of *E. coli* into stationary phase (*29*). This implies that DosC and DosP serve to integrate information about O_2 availability. For example, DosC and DosP might signal a rise of O_2 within the cells due to their slowing metabolism upon entry into stationary phase; conversely, these sensors might signal a drop in O_2 from a nearly atmospheric level upon renewed metabolic activity. The response of DosP, which increases most sharply above 75 μM O_2 (roughly 30% of ambient air O_2 concentration) suggests that c-di-GMP hydrolysis will accelerate if the cellular concentration of O_2 signals an increasing equilibration of the bacterial cytoplasm with ambient air. Stewart and colleagues have beautifully demonstrated the existence of steep O_2 gradients across the thickness of biofilms grown *in vitro* (*55*, *56*). Such gradients likely control bacterial metabolism in different layers of the biofilm (*56*). Possibly DosC and DosP closely collaborate to provide positional information to nondividing bacteria in a biofilm.

Under what circumstances would the allosteric modulation of a regulatory target be preferable to a modulation of the target's cellular *concentration* via changes in transcription or translation? We propose that this depends primarily on the longevity of the target. For example, some proteins are rapidly turned over and associated with effective and dynamic rates of transcription or translation. By contrast, consider the membrane-associated cellulose synthase complex of *G. xylinus*, with c-di-GMP regulated activity. It is costly for a cell to assemble this complex. Cessation of its synthesis would only affect cellulose production after the existing complex very slowly degraded. Clearly, regulation of the cellulose synthase activity rather than its concentration is the best approach here.

In principle, the allosteric modulation of an existing enzyme should be a more rapid method of regulation than the *de novo* synthesis of this protein activity (*25*). In practice, however, *de novo* synthesis is sufficiently rapid for all but the most urgent environmental responses. Certainly the time scale for biofilm formation is slow compared to protein synthesis rates. A fast response is not always desirable. Indeed, we would argue that the dynamics of any hypoxic response should be neither too slow nor too fast. If too slow, adaptation may not happen in time to prevent damage; if too fast, drastic responses might be made to transient changes in O_2 tension that could have been safely ignored. There is no need to raise one's red blood cell count in response to being dunked; anyone can hold their breath for a minute.

What is the advantage of regulating both the generation and destruction of a second messenger in response to one environmental signal? In *E. coli*, O_2 regulation of c-di-GMP levels is accomplished by opposing synthesis and degradation activities that are both O_2-controlled. On the other hand, in *B. pertussis*, O_2 regulation of c-di-GMP levels is achieved by an O_2-modulated synthesis opposing an O_2-independent degradation (*21*). Clearly, either approach offers the same degree of control over the final equilibrium level of the c-di-GMP, but they differ dramatically in their control of the dynamics of the response. Consider the analogy of the simple laboratory water bath. In these instruments, a heater switches on whenever the temperature drops below the thermometer set point, but there is no cooling mechanism. With a sufficiently powerful heater, for example, one can reduce the time necessary to warm up from 30 to 37 °C to the point where it becomes instantaneous; however, one cannot control the time it takes the bath to cool down from 37 to 30 °C. If we add to this heater a constant cooling mechanism, we can accelerate the cooling process but at the expense of adding a large constant workload to the heater. By contrast, consider a PCR thermal cycler. The thermoelectric elements in these ingenious devices can either heat or cool, simply by reversing polarity, and they can also be completely switched off. These devices not only reach or hold any set temperature but also approach it with any desired "ramp". The application of this analogy to enzymes that make and degrade a molecule in response to a single environmental cue is evident.

ACKNOWLEDGMENT

We thank Drs. Gerald Kramer and John Teiber for the use of laboratory facilities, the Protein Chemistry and Technology Center at UT Southwestern for assistance with the MALDI-MS analysis of DosC and DosP, and Drs. Cyril Appleby, Hemant Badgandi, and Daniel A. Kunz for critical reading of the manuscript.

SUPPORTING INFORMATION AVAILABLE

Original spectra from the DosP O_2 and CO equilibrium titrations and the mathematical expressions for the fraction of total tetrameric heme protein in the deoxy, monooxy, dioxy, trioxy, and tetraoxy states. This material is available free of charge via the Internet at http://pubs.acs.org.

REFERENCES

1. Tal, R., Wong, H. C., Calhoon, R., Gelfand, D., Fear, A. L., Volman, G., Mayer, R., Ross, P., Amikam, D., Weinhouse, H., Cohen, A., Sapir, S., Ohana, P., and Benziman, M. (1998) Three cdg operons control cellular turnover of cyclic di-GMP in *Acetobacter xylinum*: genetic organization and occurrence of conserved domains in isoenzymes. *J. Bacteriol. 180*, 4416–4425.
2. Ausmees, N., Mayer, R., Weinhouse, H., Volman, G., Amikam, D., Benziman, M., and Lindberg, M. (2001) Genetic data indicate that proteins containing the GGDEF domain possess diguanylate cyclase activity. *FEMS Microbiol. Lett. 204*, 163–167.
3. Romling, U., Gomelsky, M., and Galperin, M. Y. (2005) C-di-GMP: the dawning of a novel bacterial signalling system. *Mol. Microbiol. 57*, 629–639.
4. Ross, P., Weinhouse, H., Aloni, Y., Michaeli, D., Weinberger-Ohana, P., Mayer, R., Braun, S., de Vroom, E., van der Marel, G. A., van Boom, J. H., and Benziman, M. (1987) Regulation of cellulose synthesis in *Acetobacter xylinum* by cyclic diguanylic acid. *Nature 325*, 279–281.
5. Ross, P., Mayer, R., and Benziman, M. (1991) Cellulose biosynthesis and function in bacteria. *Microbiol. Rev. 55*, 35–58.
6. Gilles-Gonzalez, M. A. (2001) Oxygen signal transduction. *IUBMB Life 51*, 165–173.
7. D'Argenio, D. A., and Miller, S. I. (2004) Cyclic di-GMP as a bacterial second messenger. *Microbiology 150*, 2497–2502.
8. Tischler, A. D., and Camilli, A. (2004) Cyclic diguanylate (c-di-GMP) regulates *Vibrio cholerae* biofilm formation. *Mol. Microbiol. 53*, 857–869.
9. Hickman, J. W., Tifrea, D. F., and Harwood, C. S. (2005) A chemosensory system that regulates biofilm formation through modulation of cyclic diguanylate levels. *Proc. Natl. Acad. Sci. U.S.A. 102*, 14422–14427.
10. Yildiz, F. H., and Visick, K. L. (2009) Vibrio biofilms: so much the same yet so different. *Trends Microbiol. 17*, 109–118.
11. Costerton, J. W., Stewart, P. S., and Greenberg, E. P. (1999) Bacterial biofilms: a common cause of persistent infections. *Science 284*, 1318–1322.

12. Romling, U., and Amikam, D. (2006) Cyclic di-GMP as a second messenger. *Curr. Opin. Microbiol. 9*, 218–228.
13. Jenal, U., and Malone, J. (2006) Mechanisms of cyclic-di-GMP signaling in bacteria. *Annu. Rev. Genet. 40*, 385–407.
14. Ryan, R. P., Fouhy, Y., Lucey, J. F., and Dow, J. M. (2006) Cyclic di-GMP signaling in bacteria: recent advances and new puzzles. *J. Bacteriol. 188*, 8327–8334.
15. Hengge, R. (2009) Principles of c-di-GMP signalling in bacteria. *Nat. Rev. Microbiol. 7*, 263–273.
16. Galperin, M. Y., Nikolskaya, A. N., and Koonin, E. V. (2001) Novel domains of the prokaryotic two-component signal transduction systems. *FEMS Microbiol. Lett. 203*, 11–21.
17. Freitas, T. A., Hou, S., and Alam, M. (2003) The diversity of globin-coupled sensors. *FEBS Lett. 552*, 99–104.
18. Ryjenkov, D. A., Tarutina, M., Moskvin, O. V., and Gomelsky, M. (2005) Cyclic diguanylate is a ubiquitous signaling molecule in bacteria: insights into biochemistry of the GGDEF protein domain. *J. Bacteriol. 187*, 1792–1798.
19. Chang, A. L., Tuckerman, J. R., Gonzalez, G., Mayer, R., Weinhouse, H., Volman, G., Amikam, D., Benziman, M., and Gilles-Gonzalez, M. A. (2001) Phosphodiesterase A1, a regulator of cellulose synthesis in *Acetobacter xylinum*, is a heme-based sensor. *Biochemistry 40*, 3420–3426.
20. Tanaka, A., Takahashi, H., and Shimizu, T. (2007) Critical role of the heme axial ligand, Met95, in locking catalysis of the phosphodiesterase from *Escherichia coli* (Ec DOS) toward Cyclic diGMP. *J. Biol. Chem. 282*, 21301–21307.
21. Wan, X., Tuckerman, J. R., Saito, J. A., Freitas, T. A., Newhouse, J. S., Denery, J. R., Galperin, M. Y., Gonzalez, G., Gilles-Gonzalez, M. A., and Alam, M. (2009) Globins synthesize the second messenger bis-(3′-5′)-cyclic diguanosine monophosphate in bacteria. *J. Mol. Biol. 388*, 262–270.
22. Sudarsan, N., Lee, E. R., Weinberg, Z., Moy, R. H., Kim, J. N., Link, K. H., and Breaker, R. R. (2008) Riboswitches in eubacteria sense the second messenger cyclic di-GMP. *Science 321*, 411–413.
23. Ryjenkov, D. A., Simm, R., Romling, U., and Gomelsky, M. (2006) The PilZ domain is a receptor for the second messenger c-di-GMP: the PilZ domain protein YcgR controls motility in enterobacteria. *J. Biol. Chem. 281*, 30310–30314.
24. Chan, C., Paul, R., Samoray, D., Amiot, N. C., Giese, B., Jenal, U., and Schirmer, T. (2004) Structural basis of activity and allosteric control of diguanylate cyclase. *Proc. Natl. Acad. Sci. U.S.A. 101*, 17084–17089.
25. Delgado-Nixon, V. M., Gonzalez, G., and Gilles-Gonzalez, M. A. (2000) Dos, a heme-binding PAS protein from *Escherichia coli*, is a direct oxygen sensor. *Biochemistry 39*, 2685–2691.
26. Simm, R., Morr, M., Kader, A., Nimtz, M., and Romling, U. (2004) GGDEF and EAL domains inversely regulate cyclic di-GMP levels and transition from sessility to motility. *Mol. Microbiol. 53*, 1123–1134.
27. Schmidt, A. J., Ryjenkov, D. A., and Gomelsky, M. (2005) The ubiquitous protein domain EAL is a cyclic diguanylate-specific phosphodiesterase: enzymatically active and inactive EAL domains. *J. Bacteriol. 187*, 4774–4781.
28. Weber, H., Pesavento, C., Possling, A., Tischendorf, G., and Hengge, R. (2006) Cyclic-di-GMP-mediated signalling within the sigma network of *Escherichia coli*. *Mol. Microbiol. 62*, 1014–1034.
29. Sommerfeldt, N., Possling, A., Becker, G., Pesavento, C., Tschowri, N., and Hengge, R. (2009) Gene expression patterns and differential input into curli fimbriae regulation of all GGDEF/EAL domain proteins in *Escherichia coli*. *Microbiology 155*, 1318–1331.
30. Botsford, J. L., and Harman, J. G. (1992) Cyclic AMP in prokaryotes. *Microbiol. Rev. 56*, 100–122.
31. Imamura, R., Yamanaka, K., Ogura, T., Hiraga, S., Fujita, N., Ishihama, A., and Niki, H. (1996) Identification of the cpdA gene encoding cyclic 3′,5′-adenosine monophosphate phosphodiesterase in *Escherichia coli*. *J. Biol. Chem. 271*, 25423–25429.
32. Simm, R., Lusch, A., Kader, A., Andersson, M., and Romling, U. (2007) Role of EAL-containing proteins in multicellular behavior of *Salmonella enterica* serovar Typhimurium. *J. Bacteriol. 189*, 3613–3623.
33. Beyhan, S., Odell, L. S., and Yildiz, F. H. (2008) Identification and characterization of cyclic diguanylate signaling systems controlling rugosity in *Vibrio cholerae*. *J. Bacteriol. 190*, 7392–7405.
34. Kuchma, S. L., Brothers, K. M., Merritt, J. H., Liberati, N. T., Ausubel, F. M., and O'Toole, G. A. (2007) BifA, a cyclic-Di-GMP phosphodiesterase, inversely regulates biofilm formation and swarming motility by *Pseudomonas aeruginosa* PA14. *J. Bacteriol. 189*, 8165–8178.
35. Mendez-Ortiz, M. M., Hyodo, M., Hayakawa, Y., and Membrillo-Hernandez, J. (2006) Genome-wide transcriptional profile of *Escherichia coli* in response to high levels of the second messenger 3′,5′-cyclic diguanylic acid. *J. Biol. Chem. 281*, 8090–8099.
36. Blattner, F. R., Plunkett, G.III, Bloch, C. A., Perna, N. T., Burland, V., Riley, M., Collado-Vides, J., Glasner, J. D., Rode, C. K., Mayhew, G. F., Gregor, J., Davis, N. W., Kirkpatrick, H. A., Goeden, M. A., Rose, D. J., Mau, B., and Shao, Y. (1997) The complete genome sequence of *Escherichia coli* K-12. *Science 277*, 1453–1462.
37. Laemmli, U. K. (1970) Cleavage of structural proteins during the assembly of the head of bacteriophage T4. *Nature 227*, 680–685.
38. Gilles-Gonzalez, M. A., and Gonzalez, G. (2005) Heme-based sensors: defining characteristics, recent developments, and regulatory hypotheses. *J. Inorg. Biochem. 99*, 1–22.
39. Zhang, W., and Phillips, G. N. Jr. (2003) Structure of the oxygen sensor in *Bacillus subtilis*: signal transduction of chemotaxis by control of symmetry. *Structure 11*, 1097–1110.
40. Vinogradov, S. N., Hoogewijs, D., Bailly, X., Mizuguchi, K., Dewilde, S., Moens, L., and Vanfleteren, J. R. (2007) A model of globin evolution. *Gene 398*, 132–142.
41. Appleby, C. A. (1978) Purification of *Rhizobium* cytochromes P-450. *Methods Enzymol. 52*, 157–166.
42. Shikama, K., and Matsuoka, A. (1989) Spectral properties unique to the myoglobins lacking the usual distal histidine residue. *J. Mol. Biol. 209*, 489–491.
43. Conti, E., Moser, C., Rizzi, M., Mattevi, A., Lionetti, C., Coda, A., Ascenzi, P., Brunori, M., and Bolognesi, M. (1993) X-ray crystal structure of ferric *Aplysia limacina* myoglobin in different liganded states. *J. Mol. Biol. 233*, 498–508.
44. Gilles-Gonzalez, M. A., and Gonzalez, G. (2004) Signal transduction by heme-containing PAS-domain proteins. *J. Appl. Physiol. 96*, 774–783.
45. Gong, W., Hao, B., Mansy, S. S., Gonzalez, G., Gilles-Gonzalez, M. A., and Chan, M. K. (1998) Structure of a biological oxygen sensor: a new mechanism for heme-driven signal transduction. *Proc. Natl. Acad. Sci. U.S.A. 95*, 15177–15182.
46. Dou, Y., Olson, J. S., Wilkinson, A. J., and Ikeda-Saito, M. (1996) Mechanism of hydrogen cyanide binding to myoglobin. *Biochemistry 35*, 7107–7113.
47. Mansy, S. S., Olson, J. S., Gonzalez, G., and Gilles-Gonzalez, M. A. (1998) Imidazole is a sensitive probe of steric hindrance in the distal pockets of oxygen-binding heme proteins. *Biochemistry 37*, 12452–12457.
48. Kurokawa, H., Lee, D. S., Watanabe, M., Sagami, I., Mikami, B., Raman, C. S., and Shimizu, T. (2004) A redox-controlled molecular switch revealed by the crystal structure of a bacterial heme PAS sensor. *J. Biol. Chem. 279*, 20186–20193.
49. Gonzalez, G., Dioum, E. M., Bertolucci, C. M., Tomita, T., Ikeda-Saito, M., Cheesman, M. R., Watmough, N. J., and Gilles-Gonzalez, M. A. (2002) Nature of the displaceable heme-axial residue in the *Ec*Dos protein, a heme-based sensor from *Escherichia coli*. *Biochemistry 41*, 8414–8421.
50. Park, H., Suquet, C., Satterlee, J. D., and Kang, C. (2004) Insights into signal transduction involving PAS domain oxygen-sensing heme proteins from the X-ray crystal structure of *Escherichia coli* Dos heme domain (*Ec* DosH). *Biochemistry 43*, 2738–2746.
51. Taguchi, S., Matsui, T., Igarashi, J., Sasakura, Y., Araki, Y., Ito, O., Sugiyama, S., Sagami, I., and Shimizu, T. (2004) Binding of oxygen and carbon monoxide to a heme-regulated phosphodiesterase from *Escherichia coli*. Kinetics and infrared spectra of the full-length wild-type enzyme, isolated PAS domain, and Met-95 mutants. *J. Biol. Chem. 279*, 3340–3347.
52. Christen, M., Christen, B., Folcher, M., Schauerte, A., and Jenal, U. (2005) Identification and characterization of a cyclic di-GMP-specific phosphodiesterase and its allosteric control by GTP. *J. Biol. Chem. 280*, 30829–30837.
53. Sousa, E. H., Tuckerman, J. R., Gonzalez, G., and Gilles-Gonzalez, M. A. (2007) A memory of oxygen binding explains the dose response of the heme-based sensor FixL. *Biochemistry 46*, 6249–6257.
54. Yoshimura, T., Sagami, I., Sasakura, Y., and Shimizu, T. (2003) Relationships between heme incorporation, tetramer formation, and catalysis of a heme-regulated phosphodiesterase from *Escherichia coli*: a study of deletion and site-directed mutants. *J. Biol. Chem. 278*, 53105–53111.
55. Borriello, G., Werner, E., Roe, F., Kim, A. M., Ehrlich, G. D., and Stewart, P. S. (2004) Oxygen limitation contributes to antibiotic tolerance of *Pseudomonas aeruginosa* in biofilms. *Antimicrob. Agents Chemother. 48*, 2659–2664.

56. Rani, S. A., Pitts, B., Beyenal, H., Veluchamy, R. A., Lewandowski, Z., Davison, W. M., Buckingham-Meyer, K., and Stewart, P. S. (2007) Spatial patterns of DNA replication, protein synthesis, and oxygen concentration within bacterial biofilms reveal diverse physiological states. *J. Bacteriol. 189*, 4223–4233.
57. Gilles-Gonzalez, M. A., Gonzalez, G., Perutz, M. F., Kiger, L., Marden, M. C., and Poyart, C. (1994) Heme-based sensors, exemplified by the kinase FixL, are a new class of heme protein with distinctive ligand binding and autoxidation. *Biochemistry 33*, 8067–8073.
58. Winkler, W. C., Gonzalez, G., Wittenberg, J. B., Hille, R., Dakappagari, N., Jacob, A., Gonzalez, L. A., and Gilles-Gonzalez, M. A. (1996) Nonsteric factors dominate binding of nitric oxide, azide, imidazole, cyanide, and fluoride to the rhizobial heme-based oxygen sensor FixL. *Chem. Biol. 3*, 841–850.
59. Quillin, M. L., Arduini, R. M., Olson, J. S., and Phillips, G. N. Jr. (1993) High-resolution crystal structures of distal histidine mutants of sperm whale myoglobin. *J. Mol. Biol. 234*, 140–155.
60. Brantley, R. E. Jr., Smerdon, S. J., Wilkinson, A. J., Singleton, E. W., and Olson, J. S. (1993) The mechanism of autooxidation of myoglobin. *J. Biol. Chem. 268*, 6995–7010.
61. Thijs, L., Vinck, E., Bolli, A., Trandafir, F., Wan, X., Hoogewijs, D., Coletta, M., Fago, A., Weber, R. E., Van Doorslaer, S., Ascenzi, P., Alam, M., Moens, L., and Dewilde, S. (2007) Characterization of a globin-coupled oxygen sensor with a gene-regulating function. *J. Biol. Chem. 282*, 37325–37340.